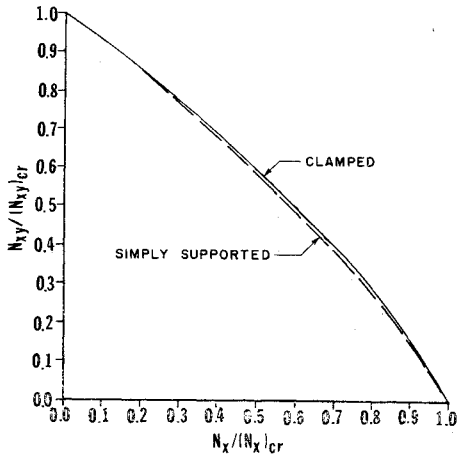

Fig. 4 Interaction curves for combined shear and axial compression for Case I of Ref. 2.

Rayleigh-Ritz solution (within 5%).[6] Some effects from the differences in assumed deflection functions and boundary conditions (see Case C-4) are seen in the slightly lower buckling load predicted by the current analysis. It was also found that by increasing the problem size from a five-term solution to an eight-term solution, the predicted buckling load decreases by 2.5%.

Case C-4 was analyzed as a result of the behavior seen in Case C-2. In this case, a similar behavior was noted, in that a very good agreement was seen in the case of panels having a very large aspect ratio and differing by as much as 10% for an aspect ratio of one. To determine the source of the difference in this case and possibly that in Case C-2, the original analysis[5] for this case was reviewed. That analysis was solved by the Lagrange multiplier method; however, explicit boundary conditions for the displacement components u and v were not presented. It is likely that they were zero at all boundaries, in which case the boundary conditions used here are slightly more flexible. This would account for the slightly lower predicted buckling load and would tend to become less significant as the panel aspect ratio increases, which is in agreement with the observed behavior. Practical shear panels have boundary conditions that fall somewhere between those of this analysis and those of Ref. 5.

In general, the buckling load depends upon twelve material and geometric parameters; thus, it is impractical to present results of a general nature. However, for the case of a flat panel without shear flexibility, the buckling load can be expressed in the dimensionless form, $K_s = (N_{xy})_{cr}b^2/\pi^2 D_y$, as a function of the dimensionless geometric parameter a/b and the two dimensionless material parameters, D_x/D_y and $\nu_{xy} + (D_{xy}/D_y)$. Using the Table 2 parameters for various composite materials, the design curves in Figs. 1 and 2 for clamped edges were calculated. For curved isotropic rectangular panels, the dimensionless design curves of Fig. 3 were generated.

Combined Shear and Axial Compression

For this combined-loading situation, only typical interaction curves were generated. These are for the glass-cloth-reinforced plastic facing, hexagonal-cell aluminum honeycomb-core panels denoted as Case I in Ref. 2. For simply-supported and clamped edges, these curves are shown in Fig. 4.

References

[1]Bert, C. W., Crisman, W. C., and Nordby, G. M., "Fabrication and Full-Scale Structural Evaluation of Glass-Fabric Reinforced Plastic Shells," *Journal of Aircraft*, Vol. 5, No. 1, Jan-Feb. 1968, pp. 27–34.

[2]Davenport, O. B. and Bert, C. W., "Buckling of Orthotropic, Curved, Sandwich Panels Subjected to Edge Shear Loads," *Journal of Aircraft*, Vol. 9, No. 7, July 1972, pp. 477–480.

[3]Davenport, O. B., "Buckling of Orthotropic, Curved, Sandwich Panels Subjected to Edge Shear and Axial Compression," M.S. thesis, Dec. 1972, University of Oklahoma, Norman, Okla.

[4]Bruhn, E. F., *Analysis and Design of Flight Vehicle Structures*, Tri-State Offset Co., Cincinnati, Ohio, p. C.12.15.

[5]Batdorf, S. B., Stein, M., and Schildcrout, M., "Critical Shear Stresses of Curved Rectangular Panels," TN 1348, May 1947, NACA.

[6]Ashton, J. E. and Whitney, J. M., *Theory of Laminated Plates*, Technomic, Stamford, Conn., 1970, pp. 61–63.

[7]Ashton, J. E., Halpin, J. C., and Petit, P. H., *Primer on Composite Materials: Analysis*, Technomic, Stamford, Conn., 1969, pp. 108–109.

[8]Pagano, N. J., "Exact Solutions for Composite Laminates in Cylindrical Bending," *Journal of Composite Materials*, Vol. 3, No. 3, July 1969, pp. 398–411.

Blockage Corrections for Large Bluff Bodies near a Wall in a Closed Jet Wind Tunnel

T. N. Krishnaswamy,* G. N. V. Rao,†
and
K. R. Reddy‡
Indian Institute of Science, Bangalore, India

Nomenclature

B	= cross section area of wake
C	= cross section area of wind tunnel
D	= drag
C_D	= drag coefficient D/qS
H, p_∞, U	= total head, static pressure and velocity of undisturbed stream
k^2	= base pressure parameter, $1-C_{p_b}$
K^2	$(k^2-1) = -C_{p_b}$
m	$= B/S$
p	= static pressure
p_b	= base pressure
C_p	= pressure coefficient $(p-p_\infty)/q$
q	= dynamic pressure of the undisturbed stream
S	= reference area of the model

Subscripts

c	= suffix denoting effective or corrected values
cc	= suffix denoting the unconstrained values far from the wall

Introduction

SINCE 1965, when a theory for the blockage effects on bluff bodies including stalled wings was published by Maskell,[1] there have been several attempts to determine the range of validity of the theory as well as other limitations if any.[2,3] There seems to be agreement now that the theory is valid up to blockages of about 8% (Ref. 4) in uniform wind beyond which, Melbourne,[2] for example, finds the similarity hypothesis $(p - p_b)/(H - p_b)$, from which Maskell worked out the blockage corrections, no longer valid. There was also clear indication that the con-

Received March 13, 1973.
Index categories: Aircraft Testing (Including Component Wind Tunnel Testing); Research Facilities and Instrumentation Safety.

*Professor. Department of Aeronautical Engineering.
†Associate Professor, Department of Aeronautical Engineering, Member AIAA.
‡Technical Assistant. Department of Aeronautical Engineering.

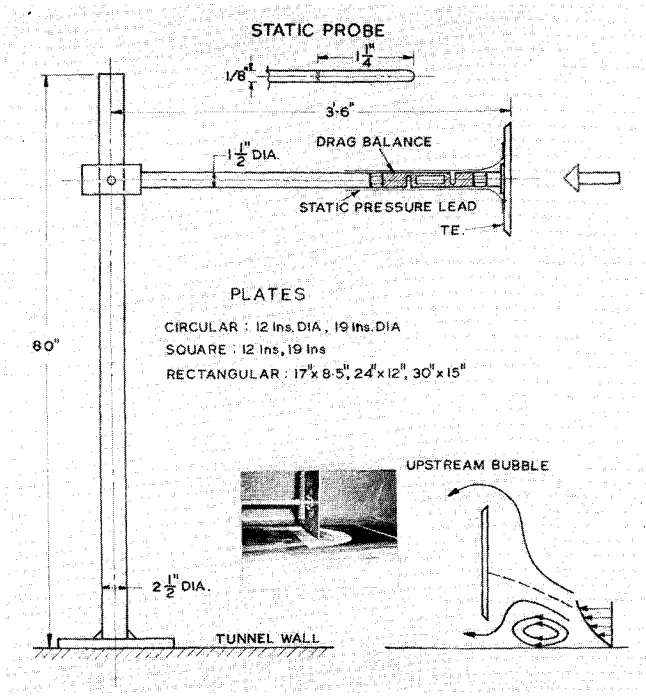

Fig. 1 Schematic of experimental setup.

stant $1/K_c^2$ in Maskell's final expression

$$C_D/C_{D_c} = 1 + C_D(S/C)/K_c^2 \qquad (1)$$

required modification. Finally, there has arisen also the need to verify the effect of the nearness of one wall on the corrections to be applied. Such problems arise in testing ground effect machine models, landing and takeoff configuration of highly swept wing aircraft, nonaeronautical structures such as antenna dishes, building models on stilts etc. In order to throw light on the nature of corrections for such conditions as well as to determine the range of validity of Maskell's correction near the center of the wind tunnel itself, a series of experiments were made on flat circular, rectangular and square disks of different sizes in three wind tunnels. The studies, which covered blockages up to 22% show that the nature of the corrections for drag envisaged in Eq. (1) holds for all distances from the wall, but that the base pressure parameter C_{Dc}/K_c^2 in Eq. (1) is a complex function of the distance from the wall. However, at the wall, it assumes a particularly simple form C_{Dc}/K_c^4.

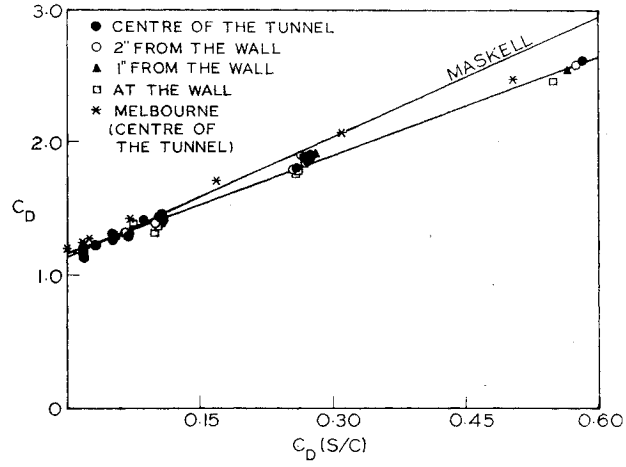

Fig. 2 Relation between C_D and $C_D(S/C)$ for different distances from the wall.

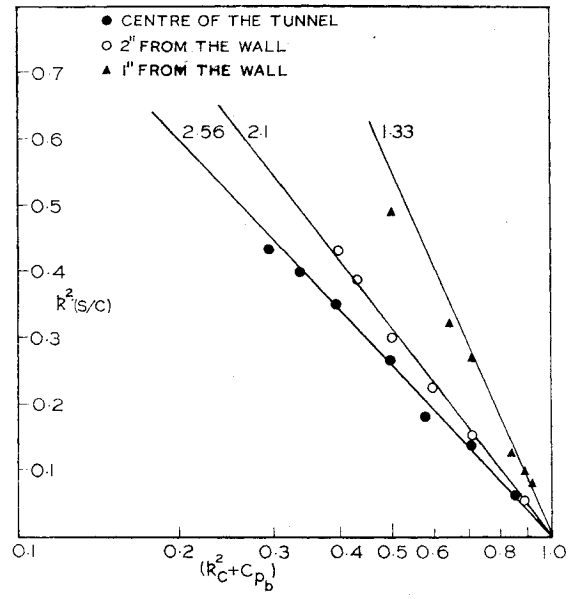

Fig. 3 Effect of proximity of the wall on base pressure parameters.

Experimental Set Up

Figure 1 shows the general arrangement used in the experiments. The three wind tunnels used were 7 × 5 ft return circuit type of elliptic cross section, 14 × 9 ft open circuit type of octogonal cross section and 9 × 6 ft return circuit type of octagonal cross section. A central plate spanning the length and breadth of the 7 × 5 ft wind tunnel was used to obtain larger blockages. The models were made from ¼ in. thick mild steel plates whose edges had been chamfered by 45° in the downstream direction. Before each test, the flow dynamic pressures in the region where the model was to be located was calibrated. A check was made in the 7 × 5 ft tunnel to ensure that the upstream influence of the model did not affect the normal reference pressures on tunnel walls in all tunnels as well as to take account of any deflection of the flow underneath the central plate (the difference in the flow above, with and without a model below was negligible). Drag was measured by a specially made strain gauge drag balance located just behind the model as shown in Fig. 1 while the

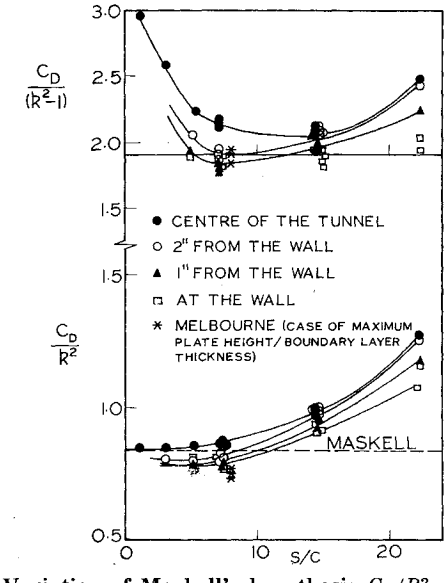

Fig. 4 Variation of Maskell's hypothesis C_D/R^2 and present hypothesis $C_D/(R^2-1)$ with blockage.

base pressures were measured by averaging the static pressure readings of four static tubes at the base, connected to an inclined (30°) alcohol manometer. The measurements quoted are the averages obtained at three speeds (typically 70, 90 and 100 fps).

Results and Discussions

Figure 2 shows the variation of C_D vs $C_D(S/C)$ from the present and the earlier data. It is observed that this relation tends to be a straight line within experimental scatter up to the maximum blockage tried, regardless of the nearness of one wall and the geometric shape of the body. The slope of the straight line fitted here is slightly less than the value given by Maskell on the basis of data for up to only 5% blockage but the linear relation seems to be hardly in doubt. This relation in general can be written as

$$C_D = C_{D_c} + 0.8C_{D_c}C_D(S/C)/K_{cc}^2 \quad (2)$$

It is also observed that C_{Dc} is practically independent of the distance from the wall but that K_c^2 changes significantly as the wall is reached. This variation is shown in Fig. 3 where $[k_c^2 + C_{pb}]$ is plotted against $k^2(S/C)$. The relation is observed to be an exponential of the form

$$C_{p_b} = -k_c^2 + \exp(-A_2k^2(S/C)) \quad (3)$$

It is obvious that for small (S/C) at the center of the wind tunnel, Eq. (3) must be compatible with Eq. (2) with (C_D/k^2) constant. A further check in fact shows that A_2 is very closely 0.8 C_{Dc}/K_c^2 so that

$$C_{p_b} = -k_c^2 + \exp(-0.8C_{D_c}k^2(S/C)/K_c^2) \quad (4)$$

Assuming the similarity of the parameter $(p - p_b(1)/(H - p_b)$ under constraint, Maskell showed that a straightforward application of momentum balance yields, with a few plausible assumptions, a linear relation between C_D and $C_D(S/C)$ for small (S/C). The fact that this is valid for blockages up to 20% indicates that the significant local departure of pressure at a point, from the similarity, tends to even out in the integrated pressure differential.

The quantity $[C_{Dc}/K_c^2]$ was found to be independent of the ratio of model size to boundary-layer thickness (about 2 in.) in our experiments, depending only on the fraction of the boundary-layer thickness at which the bottom edge of the plate was located. Closer to the wall and at the wall, when an upstream bubble was presumably formed (Fig. 1), Eq. (3) could be described by the simpler relation:

$$C_{p_b} = C_{p_{bc}} + (C_{D_c}/K_c^4)C_{p_b}(S/C) \quad (5)$$

It is therefore observed that the base pressure variation depends on the three regimes namely the uniform upstream, shear flow, and proximity to wall. A plot of C_D/k^2 and C_D/K^2 is shown in Fig. 4 where it is observed that the range of (S/C) over which Maskell's Hypothesis is valid seems to decrease with increased nearness to the wall as would be implied also from Eqs. (2) and (4). On the other hand, the quantity C_D/K^2 tends to a constant value for all (S/C) tried as the wall is reached. Thus it is observed that while far from the wall, the hypothesis that C_D/k^2 is constant is valid for small S/C, $C_D/(k^2 - 1)$ is constant at and very close to the wall. The latter condition implies that very near and at the wall $(p - p_b)/(p_\infty - p_b)$ remains invariant under constraint. Clearly the velocity scale is not the shear layer velocity kU_0 found by Maskell far from the wall, but depends on the dynamic pressure differential $[((1/2)\rho U_0^2 - (1/2)\rho k^2 U_0^2]$, K^2 being presumably related to the reattachment velocity.

Following Maskell,[1] one can derive the expression for drag coefficient of the body under constraint as

$$C_D = m\{k^2 - [C/(C - B)]\} \quad (6)$$

[Maskell's Eq. (8) simplified]. From the condition that

$$C_D/K^2 = C_{D_c}/K_c^2 = m\{k^2 - [C/(C - B)]\}/K^2 = m_c \quad (7)$$

one can derive for small S/C, assuming that $m = aK^2$,

$$C_D = C_{D_c} + (C_{D_c}C_D(S/C)/K_c^4) \quad (8)$$

$$K^2 = K_c^2 - (C_{D_c}C_{p_b}(S/C)/K_c^4) \quad (9)$$

In the present experiments, C_{Dc} 1.15 and $K_c^2 \approx 0.66$, giving $C_{Dc}/K_c^4 = 2.65$ compared with the experimentally observed value of 2.56. As Maskell has pointed out, some additional corrections due to wake distortion has to be made but this is not attempted; these corrections seem, in any case, to be small.

Application

To apply the corrections, one measures C_D and C_{pb} (*or*-K^2) and uses the pair of relations (8) and (9) for bodies on the wall, to evaluate C_{Dc} and C_{pbc} Far from the wall, Eqs. (2) and (4) can similarly be used. Elsewhere in the presence of shear, Maskell's procedure is observed to be insufficient to determine C_{Dc} and a further relation between K_c and K_{cc} is required.

References

[1] Maskell, E. C. "A Theory of the Blockage Effects on Bluff Bodies and Stalled Wings in a Closed Wind Tunnel," R&M 3400, 1965, Aeronautical Research Council, England.

[2] Melbourne, W. H. and McKeon, R. J., "Wind Tunnel Blockage Effects and Drag on Bluff Bodies in a Rough Wall Boundary Layer," Third International Conference on Wind Effects on Buildings and Structures, Vol. 1, Pt. II, 1971, Tokyo, pp. 9.1–9.9.

[3] Buckle, P. R. and Boak, A. G., "A Study of Blockage Effects of Bluff Bodies in Closed Wind Tunnels," Rept. 117, 1968, Department of Aeronautical Engineering, University of Bristol, England.

[4] Modi, V. J. and Sherbiny, S. EL. "Effect of Wall Confinement on Aerodynamics of Stationary Circular Cylinders," Third International Conference on Wind Effects on Buildings and Structures, Vol. 1 Part II, 1971, Tokyo, pp. 19.1–19.11.

Prediction of Airfoil Shock Location in Transonic Flow

Victor E. Studwell* and Jain-Ming Wu†
The University of Tennessee Space Institute, Tullahoma, Tenn.

IT is well known that a wing moving at transonic speeds will have a near normal shock wave standing near the midchord. Usually, this shock wave is coupled with a local boundary-layer separation. The shock wave location strongly influences[1] the aerodynamic force and thus the performance and stability characteristics of an aircraft.

Received May 9, 1973. This work was partially supported by The Air Force Armament Laboratory, Eglin Air Force Base, Fla., under Exploratory Development Project 2567.

Index categories: Aircraft Aerodynamics (Including Component Aerodynamics); Jets, Wakes, and Viscid-Inviscid Flow Interactions; Subsonic and Transonic Flow.

*Graduate Student and Captain, U.S. Air Force. Associate Member AIAA.

†Professor of Aerospace Engineering. Member AIAA.